Korean J. Chem. Eng., **31**(9), 1616-1623 (2014)
DOI: 10.1007/s11814-014-0072-9

pISSN: 0256-1115
eISSN: 1975-7220

Chitosan-based bioglass composite for bone tissue healing : Oxidative stress status and antiosteoporotic performance in a ovariectomized rat model

Samira Jebahi*,,†, Hassane Oudadesse*, Gada Ben Saleh*****,‡, Mongi Saoudi**,‡, Sirrar Mesadhi****, Tarek Rebai****, Hassib Keskes****, Abdelfattah el Feki**, and Hafed el Feki*****

*University of Rennes 1, UMR CNRS 6226, Campus de Beaulieu, 263 av. du Général Leclerc, 35042 Rennes, France
**Animal Ecophysiology Laboratory, Sfax Faculty of Science, Department of Life Sciences, Sfax, Tunisia
***Science Materials and Environement Laboratory, Sfax Faculty of Science, Sfax, Tunisia
****Histology, Orthopaedic and Traumatology Laboratory Sfax Faculty of Medicine, Sfax, Tunisia
*****Laboratory of Human Molecular Genetics, Faculty of Medicine, University of Sfax, Sfax, Tunisia
(*Recevied 21 June 2013 • accepted 27 February 2014*)

Abstract−Tissue engineering has opened up a new therapeutic avenue promising a revolution in regenerative medicine. Considerable attention has been given to chitosan composite materials and their applications in the field of the bone graft substitutes. We evaluated the antioxidative properties of chitosan-doped bioactive glass (BG-CH) with 17 wt% chitosan, and their applications in the guided bone regeneration. BG-CH was produced by a freeze-drying process and implanted in the femoral condyles of ovariectomized rats. Grafted bone tissues were carefully removed to evaluate the oxidative stress analysis, histomorphometric profile and mineral bone distribution by using inductively coupled plasma optical emission spectrometry (ICP-OES). A significant decrease of thiobarbituric acid-reactive substances (TBARs) was observed after BG-CH implantation. Superoxide dismutase (SOD), catalase (CAT) and glutathione peroxidase (GPx) activities significantly increased in ovariectomized group implanted with chitosan-doped bioactive glass (OVX-BG-CH) as compared to ovariectomized group implanted with bioactive glass (OVX-BG). The histomorphometric analysis showed that bone/tissue volume (BV/TV), osteoblast number (N.Ob) and osteoblast surface/bone surface (Ob.S/BS) were significantly higher in OVX-BG-CH group than in OVX-BG group. On the other hand, a rise in Ca and P ion concentrations in the implanted microenvironment was shown to lead to the formation/deposition of Ca-P phases. Trace elements such as Sr and Fe were detected in the newly formed bone and involved in bone healing. These results suggested that BG-CH composites could become clinically useful as a therapeutic and implantable material.

Keywords: Chitosan, Bioactive Glass, Graft Biomaterial, Osteoporosis, Antioxidative Profile, Bone Regeneration

INTRODUCTION

Synthetic bone graft substitutes based on composites consisting of a polymer and a bioactive glass (BG) material are developed in order to achieve successful bone regeneration [1,2]. Once implanted in the bone tissue, BG releases ions such as Na in the glass and begins to exchange with H_3O^+ in the biological fluids. The Ca and P are redeposited, leading to the formation of a hydroxyapatite-carbonated layer, which is very similar in composition to that of the bone mineral phase and includes organic components such as collagen fibers [3]. Although BG is apparently interesting in terms of bone repair and regeneration, it does not seem optimal in terms of therapeutic properties. However, chitosan (CH) is widely regarded as a bioactive substance with reactive functional groups [4]. It is a linear copolymer of (1-4) linked 2-acetamido-2-deoxy-d-glucopyranose and 2-amino-2-deoxy-d-glycopyroanose [5]. It is obtained by the deacetylation of its parent polymer chitin, a polysaccharide that is widespread in nature (e.g., crustaceans, insects and certain fungi) [6]. Other multiple functional properties such as drug delivery, antimicrobial activity and low immunogenicity, have provided ample opportunities for its potential applications [7]. Moreover, CH oral administration is proposed to prevent the decrease in bone mineral density (BMD) by inhibiting osteoclastic cells and preventing bone loss associated with postmenopausal osteoporosis [8]. This bone disorder can be treated with many bioactive substances such as alendronate, which is a bisphosphonate drug [9]. However, when it is associated with the jaw osteonecrosis, this treatment has a rare but serious adverse effect [10].

The association between CH and hydroxyapatite (Ca_{10} $(PO_4)_6$ $(OH)_2$) has recently been extensively described in ovariectomized (OVX) rats [11]. The differentiation and the activity of human preosteoclastic cells on Cementek® material containing 2% CH (deacetylation degree: 0.83) (Cementek®/CH) was compared to the Cementek® alone. The incorporation of CH to Cementek® does not affect the proliferation and adhesion of preosteoclasts, but prevents the osteoclastic resorption of the composite biomaterial. This CH property might positively influence bone formation and bone remodeling *in vivo* [12]. Likewise, CH+silica membranes were fabricated using a sol-gel process and, thus, osteoblasts were observed to adhere well and grow more actively on such a membrane [13]. CH tolerated the physiological bone formation, healing processes and most importantly enhanced favorably the biochemical responses thanks to its inherent stimulating properties [14]. In addition, the combination of

†To whom correspondence should be addressed.
E-mail: jbahisamira@yahoo.fr
‡This authors contributed equally to this work.

nylon-6 and CH oligosaccharides presents several benefits as it provides anti-bacterial effects [15].

All these beneficial CH effects on bone growth prompt us to incorporate this bioactive substance in BG for skeletal tissue applications. In this regard, Oudadesse and co-authors have successfully established the association between CH and BG in the quaternary system (SiO_2-CaO-Na_2O-P_2O_5) called BG-CH [16]. This proposed composite has not shown cytotoxic effects on Saos2 cell cultures [17]. While *in vitro* studies can reveal the essential cell-cell interactions in the presence of BG-CH, the *in vivo* analyses are the gold standard to study the biomaterial-tissue biocompatibility. Animal models such as OVX rat exhibit most of the characteristics of human postmenopausal osteoporosis. Moreover, OVX rat minimizes some of the difficulties associated with studying the disease in humans, namely time and behavioral variability among test subjects [18]. Such a model following estrogen deficiency leads not only to bone loss, but also the decrease of oxidant defense that might stimulate osteoclastic bone resorption [19]. Therefore, we notice today a growing interest in the use of natural antioxidant agent to combat oxidative stress. Currently, there has been a great deal of research interest in the CH antioxidant activity [20]. In fact, CH has obvious scavenging activities on superoxide radical. In addition, CH scavenging mechanism is reported to be related to the fact that the free radicals can react with the residual free amino groups NH_2 to form stable macromolecule radicals, and the NH_2 groups can form ammonium groups NH^{3+} by absorbing hydrogen [21]. It is worth noting that the bone response to oxidative stress in OVX rats has been adequately studied, whereas the effects of implanted CH-doped BG on the reactive oxygen species (ROS) balance in osteoporotic model have not been addressed yet. Therefore, we investigated both osteogenic capacity and antioxidant activity of a novel CH-doped BG against free radicals induced by estrogen deficiency.

EXPERIMENTAL PROCEDURES

1. Biomaterials Synthesis

First, the BG particles were synthesized via the melting method by using appropriate amounts of calcium metasilicate, sodium metasilicate and sodium metaphosphate (Sigma, France) [22]. To synthesize BG-CH biocomposite, the CH polymer (Sigma, France) with a medium molecular weight was dissolved in 1% acetic acid aqueous solution (Sigma, France) for 2 hours at room temperature. The mixture of BG particles and CH polymer was stirred for 2 hours at room temperature using magnetic stirring at 1,200 rpm (round per minute). After eliminating surplus solution, the mixture was frozen by liquid azotes and placed into a freeze dryer for 24 hours to totally exclude solvent. The obtained composite was immersed in 10% NaOH solution for 2 hours and washed several times with deionized water to neutralize the acetic acid residues. Finally, the composite was frozen by liquid azotes and freeze-dried again for 24 hours to completely remove water. The prepared implants were sterilized by γ-irradiation from a ^{60}Co Source gamma irradiation at a dose of 25 Gy (Equinox, UK) using standard procedures for medical devices.

2. Animal Model

Female *Wistar* rats (16-19 weeks of age), obtained from the Central Pharmacy, Tunisia, and bred in the central animal house, were used in this study. They were acclimatized to their new environment for 15 days before the beginning of the study. The animals were fed on a pellet diet (Sicco, Sfax, Tunisia) and water *ad libitum*. All the animals were kept under climate-controlled conditions (25 °C; 55% humidity; 12 hours of light alternating with 12 hours of darkness). The handling of the animals was approved by the Tunisian Ethical Committee for the care and use of laboratory animals. A total number of 145 *Wistar* rats were used for the experiment. All rats were randomly divided into five groups (five per group). Group I was used as negative control without bilateral ovariectomy or surgical creation of bone defects (CT). Sixty days after bilateral ovariectomy, group II was used as a positive control (OVX). Group III was implanted with BG (OVX-BG). Whereas, group IV was implanted with BG-CH (OVX-BG-CH). The histomorphometric parameters, ICP-OES and oxidative stress were evaluated in the femoral condyle tissues of the mentioned rat groups. The last group (group V) presenting empty defects (OVX-NI) was added only for the oxidative stress analysis.

3. Surgical and Post-operative Protocol

All surgical interventions were performed under general anesthesia in aseptic conditions. Anesthesia was induced with xylazine (7 to 10 mg/kg (i.P) ROMPUN® 2%, Merial; Lyon, France) and ketamine (70 to 100 mg/kg (i.m) imalgene®, Merial; Lyon, France) depending on the body weight. The animals underwent bilateral ovariectomy. The pre-operative preparation of the surgical sites was routinely carried out by cleaning with 96% alcohol and antiseptic solutions (PROLABO; AnalaR Normapur®, France). A drilled 3-mm-diameter and 4-mm-deep hole was created on the lateral aspect of the femoral condyle using a refrigerated drill to avoid necrosis. The resulting bone defects were irrigated profusely with physiological saline solution (0.9 wt% NaCl; Ref.091214; Siphal, Tunisia) to eliminate bone debris. The drill-hole was filled with 10 mg of BG and 10 mg of BG-CH in OVX-BG group and OVX-BG-CH group, respectively. On days 15 and 30 after implant insertion, all rats were sacrificed and specimens were harvested for biological and physico-chemical evaluation.

4. Oxidative Stress Measurements

4-1. Thiobarbituric Acid Reactive Substances (TBARS) Measurements

The implanted bones of all groups were minced and homogenized (100 mg/ml) at 4 °C in 0.1 mol/*l* Tris-HCl (Sigma, France) buffer pH 7.4 and centrifuged at 3,000 ×g for 10 min. Lipid peroxidation in the tissue homogenate was estimated by measuring TBARS and expressed in terms of malondialdehyde (MDA) content, which is the end product of lipid peroxidation [23].

4-2. Antioxidant Enzyme Studies

Regarding the superoxide dismutase (SOD) activity, it was assayed by the spectrophotometric method of Marklund [24]. Glutathione peroxidase (GPx) activity was measured by the method described by Pagila and Valentine [25]. Catalase (CAT) activity was assayed calorimetrically at 240 nm and expressed as moles of H_2O_2 consumed per minute per milligram of protein, as described by Aebi [26]. The level of total protein was determined by the method of Lowry et al. using bovine serum albumin [27].

5. Inductively Coupled Plasma Optical Emission Spectrometry of Newly Formed Bone

Femoral condyles were dried for 24 hours at 65 °C. Dry femurs

(weight 0.250±0.01 g of dry sample) were then weighed accurately and placed in 25-ml tubes. Next, 2 ml of nitric acid was added. Afterwards, one milliliter of 30% H_2O_2 (Sigma, France) was placed in the tube after 10 min. The mixture volume was increased to reach 500 ml with distilled water. The working standard solutions of Ca, P, Na, Sr, Si and Fe were prepared as well as the blank one. The element concentrations were detected using ICP-OES (Ciros; Spectro Analytical Instrument, Germany).

6. The Scanning Electron Microscopy Morphological Analysis

SEM (JSM-6301F Jeol, France) was used to identify the morphological changes between bone, BG-CH and BG. The collected samples were prefixed with 2.5% glutaraldehyde solution (phosphate buffer solution, pH 7.4) (Sigma, France) overnight, and then washed with phosphate buffer solution (pH 7.4). Then, the samples were postfixed with 2% osmic acid solution (Sigma, France) (phosphate buffer solution, pH 7.4) for 90 min and dehydrated with an alcohol evaporating system. The samples were then freeze-dried with a freeze-dryer (JFD-300 Electron Optic Laboratory, France), and the process was carried out with a vapor deposition system (JFC-1200, France).

7. Histomorphometric Analysis

Implanted femoral condyles were harvested, fixed in Burdack (formalin) (Sigma, France) and refrigerated. Specimens were dehydrated using graded solutions of alcohol increasing from 70% to 100% EtOH (Siphat, Tunisia). The specimens were included in a mixture of methylmethacrylate (MMA) (PROLABO, France) and glycolmthacrylate (GMA) (PROLABO, France) without prior decalcification. 6- to 7-μm-thick sections were debited along a transverse plane using a sliding microtome (Reichert-Jung, Germany). The same histology stains were used only to study very specific biological tissue types. In our study, the modified Goldner Trichrome stained a connective tissue such as bone matrices as bone/tissue volume (BV/TV, expressed in %), osteoid/bone surface (OV/BV expressed in %), osteoclast/bone surface (Oc.S/BS, expressed in %), osteoblast surface/bone surface (Ob.S/BS, expressed in %), osteoblast number (N.Ob expressed in mm^{-2}) and mineralizing surface

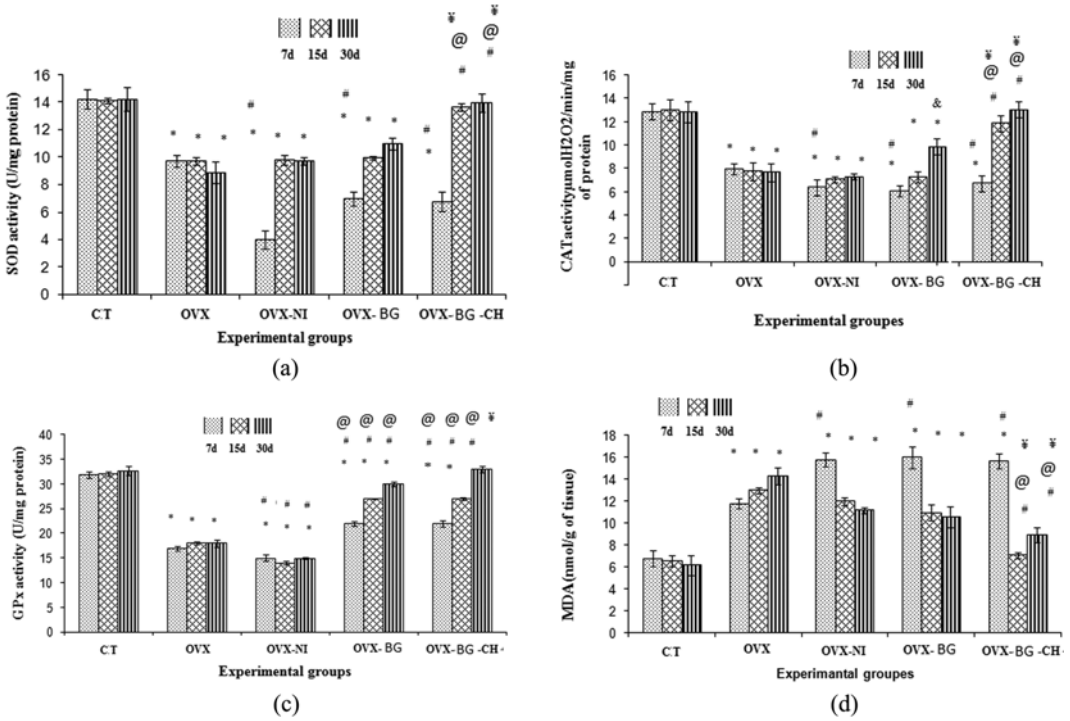

Fig. 1. (a) Effects of bioactive glass (BG) and chitosan-doped bioactive glass (BG-CH) on superoxide dismutase (SOD) activities in femoral condyle cells of ovariectomized (OVX) female *Wistar* rats for 7, 15, and 30 days. Values are given as mean±S.E. * Significantly different enzymatic activity in the indicated group than negative control group (CT). # Compared to ovariectomized group (OVX), and compared to empty defects (OVX- NI) and ¥ compared to implanted with bioactive glass group (OVX-BG). (b) Effects of bioactive glass (BG) and chitosan-doped bioactive glass (BG-CH) on catalase (CAT) activities in femoral condyle cells of ovariectomized (OVX) female *Wistar* rats for 7, 15, and 30 days. Values are given as mean±S.E. * Significantly different enzymatic activity in the indicated group than negative control group (CT). # Compared to ovariectomized group (OVX), and compared to empty defects (OVX-NI) and ¥ compared to implanted with bioactive glass (OVX-BG). (c) Effects of bioactive glass (BG) and chitosan-doped bioactive glass (BG-CH) on glutathione peroxidase (GPx) activities in femoral condyle cells of ovariectomized (OVX) female *Wistar* rats for 7, 15, and 30 days. Values are given as mean±S.E. * Significantly different enzymatic activity in the indicated group than negative control group (CT). # Compared to ovariectomized group, (OVX), and compared to empty defects (OVX-NI) and ¥ compared to implanted with bioactive glass group (OVX-BG). (d) Effects of bioactive glass (BG) and chitosan-doped bioactive glass (BG-CH) on malondialdehyde (MDA); catalase (CAT), activities in femoral condyle cells of ovariectomized (OVX) female *Wistar* rats for 7, 15, and 30 days. Values are given as mean±S.E. * Significantly different enzymatic activity in the indicated group than negative control group (CT). # Xompared to ovariectomized group (OVX), and compared to empty defects and ¥ compared to implanted with bioactive glass group (OVX-BG).

(MS/BS) were measured by a point count method [28] using a 25-point integrating filter.

8. Statistical Analysis

Statistical analysis was performed using Mann-Whitney U-test with SPSS software (Version 17.0). $P<0.05$ was accepted as statistically significant.

RESULTS

1. Measured Oxidative Stress in Bone

As illustrated in Figs. 1(a), 1(b), 1(c) and 1(d), the data on the SOD, CAT and GP_X activities in the femoral condyle of OVX rats showed a highly significant reduction when compared to those of negative controls. However, ovariectomy significantly raised the MDA levels. Similarly, after 15 days, OVX-BG-CH and OVX-BG rats revealed a highly significant decrease of SOD, GP_X and CAT activities as compared to those of OVX rats. In the beginning of the study, oxidative stress increased MDA levels in OVX-NI, OVX-BG and OVX-BG-CH rats by 58.5, 61.6 and 58%, respectively. During the 30-day implantation period, OVX-BG-CH and OVX-BG showed a particular increase in SOD, GP_X and CAT activities when compared to other groups and a significant decrease of the MDA level. This therapeutic effect was more pronounced in OVX-BG-CH than in OVX-BG group. In fact, after comparison with OVX-BG group, an increase of the SOD, CAT and GP_X activities by 23.25, 34.50 and 18% in OVX-BG-CH was shown at the end of the experiment. Moreover, a decrease in MDA by 52.3% was perceived in OVX-BG-CH as compared to that of OVX-BG group. The significant enhancement of enzymatic defense was observed mainly through the comparison with OVX groups. A pronounced increase of the SOD, CAT and GP_X activities by 40, 53.5 and 36%, respectively, was also shown. A very significant decrease in MDA by 52.3% was detected in OVX-BG-CH when compared to that in OVX group.

2. ICP-OES Characterization of Newly Formed Bone

As a result of ovariectomy, the content of Ca and P significantly decreased when compared to that of the negative control group ($P< 0.01$) as illustrated in Table 1. As regards Sr, Si, Na and Fe, no significant differences were observed when compared to those of the negative control group. The implanted group with BG-CH showed that the general reduction of Si over time is concomitant with the change in the release rate of Ca concentrations. In fact, while Si concentration decreased from 71 to 50 μg/g, Ca concentration increased from 245 to 262 mg/g. These results corroborated the P content measurements whose investigation revealed values of about 139 and 145 mg/g after 15 and 30 days, respectively. Moreover, Na content exhibited 9.00 mg/g in OVX group. These measurements indicated significant variation 30 days post surgery and represented about 12.10 mg/g in OVX-BG groups. Fe concentrations were normalized to the initial bone amount and revealed at about 715 μg/g for BG-CH group. The Sr measurements in OVX bone tissue were exhibited at about 140 μg/g. The OVX-BG-CH and OVX-BG groups showed a significant decrease of Sr and were revealed at about 122 and 109 μg/g, respectively.

3. Histological Analysis

Femoral condyle defect was characterized with a disconnected trabecular bone in the OVX on day 60 after ovariectomy (Fig. 2(a)). After 15 days, a new woven bone was still growing and filling the gap between the host bone and BG implant (Fig. 2(b)). A particular profile of gel layer adhesion to the new bone was observed in the OVX-BG-CH implanted group (Fig. 2(c)). Furthermore, histological evidence proved the presence of an osteogenic reaction and the dominance of an osteoid tissue, indicating the characteristic process involved in the formation of a new bone in OVX-BG implanted group (Fig. 2(d)). However, the dominance of the mineralized tissue in the OVX-BG-CH implanted group (Fig. 2(e)) was noted. Moreover, the level of the basic structural unit wall width and the trabecular hypertrophy indicated a pronounced increase. In fact, BG-CH was shown to limit bone loss, inducing a beneficial impact on the trabecular bone microarchitectural properties. It was confirmed by the reduced inter-trabecular space and the higher trabecular thickness when compared to those of OVX-BG-treated rats (Fig. 2(f), (g)). BG-CH was resorbable and showed the capacity to re-build the cancellous structure and replace it with a newly-formed bone in order to prevent osteoporotic femoral condyle defect. There was also an increase in the osteoblast number (Fig. 2(h)). Although the maturity of the bony matrix was marked by the important number of osteocytes enclosed in a space called the lacuna room (Fig. 2(j)), a limited number of osteoclastic cells appeared in the Howship lacunae (Fig. 2(i)). The pore networks were visualized by SEM, whose results demonstrated that BG-CH had an average pore size of approximately 10 μm in diameter. The pores could be expected to afford space for the bone in growth.

4. SEM Morphological Analysis

At the beginning of the experiment, there was no cell invasion

Table 1. Distribution of Ca, P, Si, Sr, Na, and Fe in newly formed bone of ovariectomized (OVX) female *Wistar* rats implanted with bioglass (OVX-BG) and chitosan-doped bioglass (OVX-BG-CH) for 15 and 30 days

Elemental analysis / Treatement groups		Ca (mg/g)	P (mg/g)	Si (μg/g)	Sr (μg/g)	Na (mg/g)	Fe (μg/g)
CT		250±80	141±90	25±09	141±50	9.40±90	710±90
OVX		215±70*	138±88*	24±08	140±90	9.00±90	710±90
BG	15d	260±68*	139±70	79±09*	88±3*	13.20±1*	740±2*
	30d	230±78*	137±60*	62±04*	109±2*	12.10±2*	733±3*
BG-CH	15d	262±88*	139±40	71±08*	105±4*¥	12.12±5*	720±2¥*
	30d	245±78¥	145±50*	50±07*¥	122±2*¥	10.10±4	715±3¥

* Significantly different level in the indicated group than negative control (CT) group and ¥ compared to implanted with bioglass (OVX-BG) group

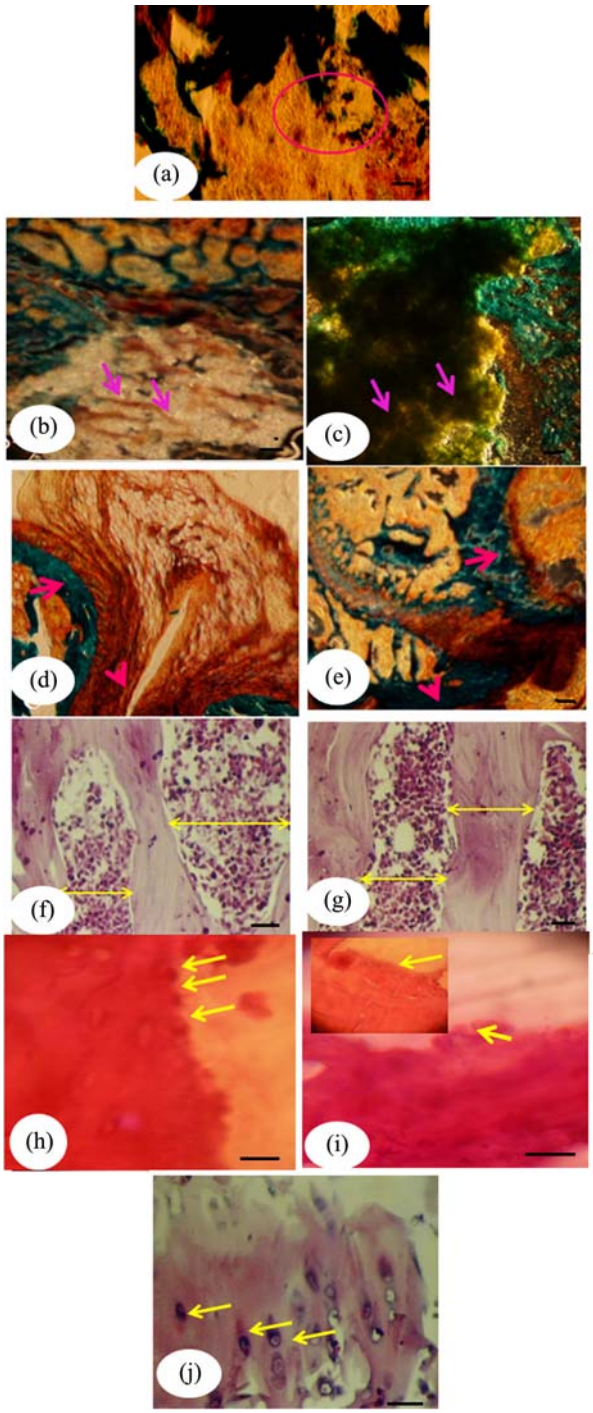

Fig. 2. A disconnected trabecular bone in the OVX at 60 days after ovariectomy (a). A new woven bone in the BG implanted group (b). A gel layer adhesion to the new bone in the OVX-BG-CH implanted group (c). The osteoid tissue in OVX-BG implanted group (d). The mineralized tissue in the OVX-BG-CH implanted group (e). A reduced inter-trabecular space and a higher trabecular thickness when compared to that of BG-treated rats (f), (g). Osteoblast cells (h). The osteocyte enclosed a space called the lacuna room (i). Osteoclastic cells in the Howship's lacunae-like (j). Goldner's trichrome staining ((a), (b), (c), (d), (e)) (10× objective). Hematoxylin and eosin stain ((f), (g), (×10) (h), (i) (×100), (j) (×40)). ((a), (b), (c), (d), (e), (f), (g): scale bar=20 μm), ((h), (i), (j): scale bar=10 μm).

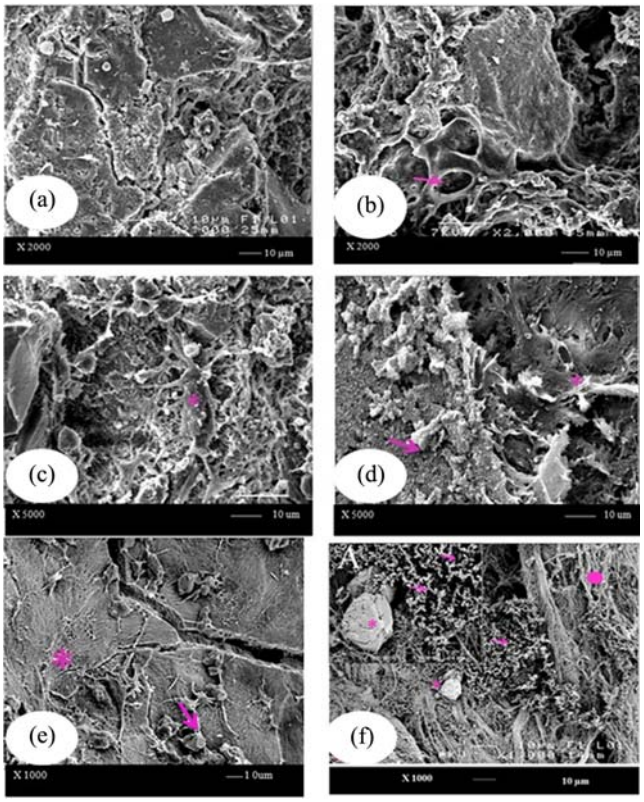

Fig. 3. Absence of cell invasion on the OVX-BG or on the OVX-BG-CH implanted groups (a), (b). Highly cellular layer, more advanced ossification and a larger stimulation of osteoregeneration surrounding OVX-BG-CH compared with those of the OVX-BG group (c), (d). Remarkable degree of bone maturation after OVX-BG-CH implantation (e). OVX-BG-CH biodegradation and mineral crystal disturbance among the collagen fibrils of bone (f).

on the OVX-BG or on the OVX-BG-CH implanted groups (Fig. 3(a), (b)). After 30 days, OVX-BG-CH was shown to encourage cell spreading. In fact, the bone surrounding BG-CH presented a highly cellular layer, more advanced ossification and a much larger stimulation of osteoregeneration than that surrounding the OVX-BG group. However, only few cells were observed on the surface of BG biomaterial group (Fig. 3(c), (d)). By the end of the experiment, the degree of the new bone maturation was so remarkable that the new bone could not be differentiated from normal bone (Fig. 3(e)). Fig. 3(f) shows the BG-CH biodegradation and the mineral crystals disturbance among the bone collagen fibrils.

5. Histomorphometric Analysis

Thirty days after surgery, the quantitative analysis demonstrated that the parameters of BV/TV, N.Ob and Ob.S/BS were significantly higher in OVX-BG-CH-treated group than in OVX-BG-treated group, which changed by 5, 25.2 and 19%, respectively. On the other hand, Oc.S/BS and OV/BV parameters decreased considerably in the OVX-BG-CH-treated group when compared to those in OVX-BG-treated rats by 39.7 and 35.75%, respectively (Table 2).

DISCUSSION

Research work on bone regeneration with the aid of bone cements

Table 2. Determination of (BV/TV) (A), (N.Ob) (B), (Ob.S/BS) (C), (OV/BV) (D), (Oc.S/BS) (E) after 15 and 30 days in control femoral condyle *Wistar* rats (CT), ovariectomized (OVX), and filled with bioglass and bioglass-doped chitosan (OVX-BG and OVX-BG-CH)

Histomorphometric parametrs \ Treatement group		CT	OVX	OVX-BG	OVX-BG-CH
BV/TV%	15d	35.00±09	21.00±1.1*	46.50±11*	43.00±11#
	30d	35.00±10	20.90±10*	40.00±12#	38.00±09#
N.ob (mm-3)	15d	44.00±14	30.00±16*	33.50±13*	38.00±10#
	30d	43.00±18	26.9±15*	34.40±14*	46.10±12¥#
Ob.S/BS%	15d	3.5±0.01	4.8±0.14*	2.99±0.12*#	2.9±0.16#
	30d	3.6±0.02	5.33±0.13*	2.60±0.11*#	3.2±0.13#
OV/BV%	15d	0.2±0.01	0.6±0.03*	0.52±0.04*#	0.51±0.03*#
	30d	0.2±0.03	0.68±0.04*	0.53±0.04*#	0.32±0.04¥
Oc.S/BS%	15d	0.8±0.06	1.5±0.1*	1.4±0.3*	1.2±0.1*
	30d	0.8±0.07	1.6±0.2*	1.4±0.2*	0.91±0.5¥

* Significantly different in the indicated group than that of CT group. # Significantly different compared to ovariectomized group (OVX), ¥ Compared to implanted with bioglass (OVX-BG) group

has recently become more refined in terms of the healing process. In fact, CH has intensively been studied in pharmaceutical applications as a bioactive additive with gel-forming capability, high adsorption capacity and biodegradability. Although the focus on CH as a reactive functional group associated with BG is of interest, its antioxidative profile during the bone healing has not been reported in research work. We OVX rats are used as a metabolically altered bone model to improve the beneficial effect of BG-CH biomaterial. The analyses have demonstrated an increase of MDA level in OVX-treated rats showing excessive lipid peroxidation (LPO) levels in bone tissue. Moreover, the results show that in OVX-treated rats, this change is accompanied with a concomitant decrease in the antioxidant enzyme activities such as SOD, CAT and GPx. Indeed, after ovariectomy, the excessive production of the ROS could be regarded as a result of free radicals generated by estrogen deficiency. The mechanisms through which estrogen deficiency stimulates bone resorption remain controversial [29]. Estrogen is shown to exert beneficial actions by ROS suppression [30]. Its insufficiency motivates ROS to stimulate osteoclast cells [30].

In the present study, 30 days following BG-CH administration, the MDA level intensity regained the normal value in OVX-BG-CH-treated rats. However, a weak antioxidant activity was detected after BG administration during this period. On the other hand, the NI group exhibited pro-oxidant effect without a significant decrease in the MDA concentration production in comparison with those of all other treated groups. This may be accredited to the BG-CH metabolic stimulation and reparative processes, which suggests that this composite can modulate the balance of antioxidants and prooxidants one month after surgery. Some characteristics, such as the chelation of some free metal ions, enable CH to inhibit the lipid oxidation of many foods [31].

According to the literature, there is an increase in the free radical scavenging activity of CH, which is irradiated at a dose up to 30 kGy of gamma radiation. This is probably due to the increased exposure of free amino groups during the CH depolymerization after irradiation [32]. As reported, the CH antioxidant activity is mainly attributed to the hydroxyl and amino groups and is considered as an important factor that may delay lipid oxidation by chelating ferrous ions, thus eliminating their prooxidant activity or their conversion to ferric ion [33]. On the other hand, the CH inhibitory mechanism on free radicals may be ascribed to the amine groups for chelating Cu^{2+}, which is a reagent element in the Fenton reaction [34]. This chelating effect on Cu^{2+} may inhibit the generation of hydroxyl radicals. As reported, CH might affect the endogenous antioxidant levels that might be up-regulated by the increased expression of the genes encoding the antioxidant enzymes SOD, CAT or GPx [35]. In the present study, the introduction of 17 wt% CH in BG material represents an efficacious source of natural antioxidants able to function in the regenerated bone tissue. However, the therapeutic function of CH is not only limited to the excessive activity of scavenging free radicals but can also accelerate bone repair and ameliorate the bone trabecular structure awakened by osteoporosis. In a recent study, freeze-dried porous γ-tricalcium phosphate+CH composites with 120 μm pore size and 91.07% porosity have shown a higher proliferation rate than the pure CH, and upregulated the gene expression of bone sialoprotein attachment protein. Another study tried to improve bone tissue reconstitution with CH+calcium phosphate composites on rabbit and sheep model [36]. In fact, histological evidence has proven the presence of an osteogenic reaction moving from the rim of the surgical lesion toward the center. In controls, dense fibrous tissue deprived of the bone characteristic histoarchitecture can be observed [37]. In the current study, two weeks after bone implantation, a new woven bone synthesis occurred through an appositional growth mechanism. Woven bone is found only in cases of trauma or disease, most frequently occurring around bone fracture sites. It is laid down rapidly, thus explaining its disorganized structure. Woven bone is believed to be less dense because of the loose and disorganized packing of type I collagen fibers [38]. Four weeks later, a big defect was being invaded by trabecular tissue. A huge fragmentation and integration of the BG-CH implant could be seen between the bone defect tissues. The circulating progenitor bone cells could be hosted by the BG-CH implant, i.e., they assem-

bled on the pre-existing bone and deposited new layers of collagen-rich extracellular matrix, which were subsequently mineralized few weeks after surgery as shown in Fig. 2(f). The BG-CH bone graft seems to enhance new bone tissue ingrowth and reinforce the trabecular structures, which may control the excessive resorption activity of osteoclasts. Herein, the measured histomorphometric parameters show that BG-CH has an important capacity to influence both mineralization and cell activity, which is proven to be successful and prompt bone healing. In fact, a significant variation of BV/TV was clearly detected with BG-CH implant. In addition, N.Ob and Ob.S/BS increased to 25.2 and 19% in OVX-BG-CH groups when compared to those in OVX-BG group, respectively. Herein the CH supplementation to BG presents an efficacious therapy for the bone rarefaction caused by the hormonal insufficiency. Four weeks after surgery, BG-CH was shown to induce intensive remodeling with the highest affinity to the bone receiving BG biomaterial. The experimental data confirmed that BG materials alone were unable to locally rebalance significantly the osteoclastic and osteoblastic activities in this induced form of osteoporosis. In this study, BG-CH was suitable for bone repair and regeneration because after implantation in bone defects, it was rapidly integrated into the bone structure, and then it was transformed into new bone thanks to the activity of osteoclasts and osteoblasts. This composite filled the bone defect and permitted subsequent osteointegration. When applied to surgical femoral defects, BG-CH generated a novel histoarchitectural order in the newly formed bone within four weeks, and the spongious trabecular architecture was restored. Moreover, the decrease in bone volume fraction that is classically described between normal and osteoporotic bones [39] was not significantly modified in BG group and did not compensate efficaciously the bone microarchitectural disorder. By the end of the experiment a very important similarity was observed between the treated femurs and the healthy ones, demonstrating the spectacular efficiency of the combined system (CH and BG) in the considered animal. In fact, these positive microarchitectural alterations were confirmed by SEM observations, which revealed a densification of the bone network. As an explanation of this important osteoproductive capacity, some studies have demonstrated that CH positive charge allows for electrostatic interactions with glycosaminoglycans, which attracts growth factors that enhance cell growth and proliferation [40].

All these results have revealed the BG-CH ability not only to form new bone but also to reinforce the existing trabecular bone in the osteoporotic site. We also investigated the mineral profile of the regenerated bone. In fact, four weeks after surgery, the Ca measurements in the newly-formed bone indicated the deposition of significant amounts of mineralized matrix, with a significant increase of Ca-P. This layer indicated the BG-CH bioactivity. Such a composite formed a chemical bond with the bone tissue resulting in a very strong bone/BG-CH interface. However, the influence of some composites on the structure of the HA-like conversion product remains unclear [41]. On the other hand, Fe trace content, performed in BG-CH-bone area, revealed the presence of cavities previously filled with red blood cells. BG was degraded so as to release Na and soluble silica, presumably in the form of Si $(OH)_4$. It is believed that the combination of some of these ions triggers cells to produce new bone [42]. The lack of a reactive or a granulomatous inflammatory reaction in bone tissue with BG-CH and BG by the end of the treatment proved the absence of pathological abnormalities which support the local and systemic BG-CH histocompatibility. In fact, previous research studies have reported that CH exhibits various pharmacological actions. They have also shown that CH can gradually depolymerize to release N-acetyl-β-D-glucosamine, which initiates fibroblast proliferation [43] and helps in the ordered collagen deposition at the wound site. Moreover, it induces inflammatory cell migration and angiogenetic activity favoring a high neo-tissue vascularization. Furthermore, CH regulated secretion of the inflammatory mediators such as interleukin 8, prostaglandin E and interleukin 1 β [44]. The present results have shown that CH can promote cell proliferation and accelerate bone repair as compared to BG implant. Another study has proven that osteoblast-like cells on CH+ poly (L-lysine) present a better-developed cytoskeletal organization and higher adhesion, proliferation and differentiation than those on CH. Moreover, they achieved enhanced mRNA expression of fibronectin, integrin-$\alpha 5$, and integrin-$\beta 1$, thus qualifying for use in guided bone regeneration.

Based on these results, the incorporation of 17%W of CH in BG tolerates physiological bone formation and improves the bone architecture and the healing processes. CH is simultaneously effective in promoting mineralization and cell activation. Most importantly, CH might be considered as an adjunct therapeutic strategy. This bioactive composite contributes to combating the oxidative process by favorably enhancing the biochemical responses (antioxidative enzymes SOD, CAT and GPx). Therefore, BG-CH might be considered as an effective biomaterial to protect living organisms against ROS. BG-CH can be regarded as a promising biomaterial for tissue healing, antioxidant and regenerative therapies.

REFERENCES

1. G. Tan, M. A. Onur and N. Sağlam, *Turk. J. Biol*., **36**, 621 (2012).
2. M. J. Lee, D. Y. Seo, H.-E. Lee and G. J. Choi, *Korean J. Chem. Eng*., **28**, 1411 (2011).
3. L. L. Hench and H. A. Paschall, *J. Biomed. Mater. Res.*, **7**, 42 (1973).
4. M. Ul-Islam, N. Shah, J. H. Ha and J. K. Park, *Korean J. Chem. Eng*., **28**, 1743 (2011).
5. M. Dasha, F. Chiellinia, R. M. Ottenbriteb and E. Chiellinia, *Prog. Polym. Sci*., **36**, 1014 (2011).
6. N. V. Majeti and R. Kumar, *React. Funct. Polym*., **46**, 27 (2000).
7. S. Jarudilokkul, A. Tongthammachat and V. Boonamnuayvittaya, *Korean J. Chem. Eng*., **28**, 1251 (2011).
8. H. Iwata, S. Yana, M. Nasu and T. Yosue, *Oral. Radiol*., **21**, 22 (2005).
9. Kučukalić-Selimović E, Valjevac A, Hadžović-Džuvo A, Skopljak-Beganović A, Alimanovic-Alagić R and Brković A, *Bosn. J. Basic. Med. Sci*., **11**, 5 (2011).
10. K. E. Song, Y.-K. Min, J.-K. Lee, K. B. Lee, H. J. Joo, K.-S. Kwack and Y. S. Chung, *Curr. Therap. Res*., **69**, 36 (2008).
11. N. Rochet, T. Balaguer, F. Boukhechba, J. P. Laugier, D. Quincey, S. Goncalves and G. F. Carle, *Biomaterials*, **30**, 7 (2009).
12. G. M. Luz and J. F. Mano, *Biomed. Mater*., **7**, 054104 (2012).
13. J. Mota, N. Yu, S. G. Caridade, G. M. Luz, M. E. Gomes, R. L. Reis, J. A. Jansen, X. F. Walboomers and J. F. Mano, *Acta Biomater*., **8**, 80 (2012).

14. R. Belalia, S. Grelier, M. Benaissa and V. Coma, *Agric. Food Chem*., **56**, 8 (2008).
15. S. S. Al-Deyab, M. H. El.Newehy, R. Nirmala, A. Abdel-Megeed and H. Y. Kim, *Korean J. Chem. Eng*., **30**, 428 (2013).
16. X. V. Bui, H. Oudadess, Y. Le Gal, O. Merdrignac-Conanec and G. Cathelineau, *Korean J. Chem. Eng*., **29**, 220 (2012).
17. H. Oudadesse, X. V. Bui, Y. Le Gal, A. Mostafaand and G. Cathelineau, *Int. J. Biol. Biomed. Eng*., **5**, 56 (2011).
18. T. T. Russell, A. Maran, S. Lotinun, T. Hefferan, G. L. Evans and M. Zhang, *Rev. Endocr. Metab. Dis*., **2**, 127 (2001).
19. K. K. Lam, P. Y. Cheng, G. Hsiao, S. Y. Chen, H. H. Shen, M. H. Yen and Y. M. Lee, *Am. J. Hypertens*., **22**, 34 (2009).
20. E. B. Kurutas, A. Sahan and T. Altun, *Turk. J. Biol.*, **33**, 282 (2009).
21. F. Tian, Y. Liu, K. Hu and B. Zhao, *J. Mater. Sci*., **38**, 4712 (2003).
22. H. Oudadesse, E. Dietrich, Y. L. Gal, P. Pellen, B. Bureau, A. A. Mostafa and G. Cathelineau, *Biomed. Mater*., **6**, 035006 (2011).
23. J. A. Buege and S. D. Aust, *Methods Enzymol*., **105**, 310 (1984).
24. S. Marklund and G. Marklund, *Eur. J. Biochem*., **47**, 474 (1975).
25. D. E. Pagila and W. N. Valentine, *J. Lab. Clin. Med*., **70**, 169 (1967).
26. H. Aebi, *Methods Enzymol*., **105**, 126 (1984).
27. O. H. Lowry, N. J. Rosebrough, A. L. Farr and R. J. Randall, *J. Biol. Chem*., **193**, 275 (1951).
28. R. K. Schenk, W. A. Merz and J. A. Müller, *Acta Anat*., **74**, 53 (1969).
29. J. M. Lean, J. T. Davies, K. F. Christopher, J. B. G. Kirstein, A. Partington, Z. L. Urry and T. J. Chambers, *Am. Soc. Clin. Invest*., **112**, 923 (2003).
30. S. Muthusam, I. Ramachandran, B. Muthusamy, G. Vasudevan, V. Prabhu, V. Subramaniam, A. Jagadeesan and S. Narasimhan, *Clin. Chim. Acta*, **360**, 6 (2005).
31. F. Shahidi, J. K. V.Arachchi and Y. J. Jeon, *Trends. Food Sci. Technol*., **10**, 51 (1999).
32. T. Ur Rashid, M. M. Rahman, S. Kabir, S. M. Shamsuddin and M. A. Khan, *Polym Int*., **61**, 1308 (2012).
33. Y. C. Chung, C. L. Kuo and C. C. Chen, *Bio Technol*., **96**, 1482 (2005).
34. R. F. Del Maestro, J. Björk and K. E. Arfors, *Microvasc Res*., **22**, 70 (1981).
35. K. Regnström, E. G. Ragnarsson, M. Fryknäs, M. Köping-Höggard and P. Artursson, *Pharm. Res*., **23**, 482 (2006).
36. J. E. Maté-Sánchez de Val, P. Mazón, J. L. Guirado, R. A. Ruiz, M. P. B. Negri, M. Abboud and P. N. De Aza, *J. Biomed. Mater. Res. A*. (2013). [Epub ahead of print]
37. N. Arya, V. Sardana, M. Saxena, A. Rangarajan and A. Katti, *J. R. Soc. Interface*., (2012). [Epub ahead of print]
38. M. Doblaré and J. M. García, *Acta Cient. Venez*., **54**, 58 (2003).
39. P. L. Mente and J. L. Lewis, *J. Orthop. Res*., **7**, 461 (1989).
40. E. Verrona, O. Gauthiera, P. Janvierc, P. Pileta, J. Lesoeura, B. Bujolic, J. Guicheux and J. M. Bouler, *Biomaterials*, **31**, 84 (2010).
41. M. N. Rahaman, D. E. Day, B. S. Bal, Q. Fu, S. B. Jung, L. F. Bonewald and A. P. Tomsia, *Acta Biomat*., **7**, 2373 (2011).
42. S. Jebahi, H. Oudadesse, H. El Feki, T. Rebai, H. Keskes, P. Pellen and A. El Feki., *J. Appl. Biomed*., **10**, 209 (2012).
43. R. Jayakumar, M. Prabaharan, P. T. Sudheesh Kumar, S. V. Nair and H. Tamura, *Biotechnol. Adv*., **29**, 37 (2011).
44. A. Denuzière, D. Ferrier and A. Domard, *Ann. Pharm*., **58**, 53 (2000).